Int. J. Heat Mass Transfer. Vol. 14, pp. 835–857. Pergamon Press 1971. Printed in Great Britain

HEAT TRANSFER IN LIQUID-FLUIDIZED BEDS†

E. ZAHAVI‡

Technion—Israel Institute of Technology, Haifa, Israel

(*Received* 19 *January* 1970 *and in revised form* 24 *September* 1970)

Abstract—There exist two pertinent heat transfer modes in a fluidized bed: one—convective heat transfer between points of the bed, caused by particles' mixing; and the other—surface heat transfer between particles and fluid. The two modes produce an effective heat conduction, or diffusion, in the fluidized bed. In order to predict the temperatures in the fluidized bed, the knowledge of the effective thermal diffusivity is necessary. The achieved objectives of the present research are: (a) theoretical explanation of the heat transfer; (b) experimental determination of the said diffusivity.

The work is divided into two main parts, experimental and theoretical. In the experimental part, the effective thermal diffusivity values are obtained by means of a fluidized bed test apparatus. The obtained values fit the semi-empirical correlation developed later in our theoretical analysis

$$\frac{\kappa_{\text{eff}}}{\nu_f} = C \cdot \frac{\rho_s c_s}{\rho_f c_f} \cdot \frac{Re^{*0.25}}{Pr^{0.75}}$$

where Re^* is a Reynolds number based on the particle's diameter and the root mean square fluctuation velocity defined by equation

$$(\sqrt{\overline{u'^2}}) = 1.21 \frac{(gd)^{0.5}}{(1-\varepsilon)^{0.33}} \cdot \left(1 - \frac{\rho_f}{\rho_s}\right)^{0.5}.$$

C is a proportionality factor. By plotting the test data it is found that $C = 5320$. The test data fit the above equation with a standard deviation ± 34 per cent.

In the theoretical part of work, an analysis of the heat transfer caused by particle mixing is performed by means of the theory of stochastic processes. It is shown that with certain simplifying assumptions the heat transfer process becomes a Wiener process. From the theory of Wiener processes it is found that the effective thermal diffusivity of fluidized bed is a function of the mean kinetic energy of particle and the heat-transfer coefficient. To complete the analysis, the expressions of the mean kinetic energy of particle and the heat transfer coefficient are developed. Both expressions in conjunction with the theory of Wiener processes produce the semi-empirical correlation shown above.

NOMENCLATURE

A,	particle surface;
a,	constant;
b,	constant;
C,	empirical constant;
c,	specific heat:
c_D,	drag coefficient;
D,	column diameter; drag in equation (75);
d,	particle diameter;
E	energy of particle;
F,	stochastic function;
f,	function; friction factor in equation (53);
G,	flow rate;
g,	gravity constant;
H,	holdup;
h,	heat-transfer coefficient;
j,	Colburn factor;

† This research was carried out under the supervision of Prof. A. Kogan at the Department of Aeronautical engineering, Technion—Israel Institute of Technology, in a partial fulfilment for the D.Sc degree.

‡ Present address: University of the Negev, Beer-Sheva, Israel.

K, stochastic function;
k, thermal conductivity; constant in equation (8);
L, length of test tube;
l, length; constant in equation (8);
m, mass of particle;
N, number of particles;
P, force;
p, probability function; pressure in equations (76) (78);
S, sum of squares; stochastic function in equation (6);
T, temperature;
t, time;
U, velocity in Lagrangian system;
u, velocity;
V, volume of particle: V_B volume of fluidized bed;
W, weight;
X, coordinate in Lagrangian system;
x, coordinate.

Greek symbols

α, friction factor;
γ, factor defined by equation (64);
δ, dissipation length; δ_1 Kolmogorov's microscale;
ε, void fraction;
κ, thermal diffusivity;
ν, kinematic viscosity;
ρ, density;
σ, specific particle surface;
ϕ, stochastic function; function in equation (1);
χ, diffusivity.

Dimensionless groups

Nu, Nusselt number;
Pr, Prandtl number;
Re, Reynolds number.

Subscripts

a, solids in hopper 1;
B, fluidized bed;
eff, effective;
f, fluid;
i, space direction;
j, space direction;
L, location $x = L$;
m, molecular;
s, solid;
v, test reading;
0, location $x = 0$; slip velocity (u_0 only);
1, 2, 3, space directions; locations.

Other symbols

$\bar{}$, (overbar) mean;
$\sim$, superficial;
$'$, (prime) derivative; fluctuation (T' and u' only);
$*$ (asterisk) as defined in equation (89).

Bold symbols indentify vectors.

1. INTRODUCTION

FLUIDIZED beds by their very nature make ideal heat exchangers. They possess large heat-transfer area, high heat exchange effectiveness, and a simple design which keeps the construction costs low. All of this enhances the application of fluidized beds in heat exchange processes of the chemical industry and make the fluidized beds a technological success. Now the fluidized beds are looked upon as a possible solution to the problem of heat recovery in flash distillation plants. The first attempts in this direction were restricted to the liquid–liquid fluidized bed heat exchangers. A new application is under investigation in this faculty which uses solid–liquid fluidized beds (see [1]).

The new heat exchanger comprises a countercurrent solid–water fluidized bed. Its development depends upon the knowledge of the solid–fluid heat transfer. Now the available heat-transfer information in this field could not be used because the data obtained by the previous investigators were in conflict. Discrepancies of published data and inconsistent explanations of the heat-transfer mechanism prompted the present research.

The following two objectives constitute the subject of this work: (a), to understand the heat-transfer mechanism in a fluidized bed; and (b), by experimental means to obtain the necessary heat transfer parameter. The work is divided into two parts, experimental and theoretical. In the experimental part we obtain the necessary heat transfer parameters. In the theoretical part the mechanism of heat transfer in fluidized bed is explained. For the reader's convenience, the present paper comprises three main sections: first, the state of art of fluidized beds, described in Section 2; second, our experimental methods, described in Section 3; third, the theoretical investigation, described in Sections 4 and 5. In addition, in Section 6 our results are compared with those of others.

2. STATE OF ART

To understand the heat transfer between fluidized particles and fluid, one has to know the state of the fluidized bed as a whole as well as the fluid flow past the individual particles. The following three subsections (2.1–2.3) show the existing state of art in literature prior to the publication of the present study.

2.1. *Fluidized bed*

Two fundamental approaches are shown in the literature on this subject [2, 3], both are inter-related. We shall analyze [2] first. Consider a fluidized bed where the solid particles are suspended by fluid stream. It is evident that void fraction ε or the frequently used holdup $H = 1 - \varepsilon$ depends upon the fluid rate which suspends the particles. An increase in the fluid rate will decrease the holdup and vice versa. If we introduce the slip velocity u_0 which is the mean velocity through the voids, this dependence can be expressed as

$$H = 1 - \varepsilon = \phi(u_0) \tag{1}$$

where $\phi(u_0)$ means a function of u_0. The function depends upon the properties of fluid and solids and is being determined experimentally. Figure 1 shows a typical function $\phi(u_0)$ taken from [4].

Consider a fluidized bed contained in a vertical column where the bulk of particles is no longer suspended but flows downward with the mean velocity u_s, and the fluid flows upward with the velocity u_f. Assume the upward direction as positive, i.e. $u_f > 0$ and $u_s < 0$. Evidently,

$$u_0 = u_f - u_s. \tag{2}$$

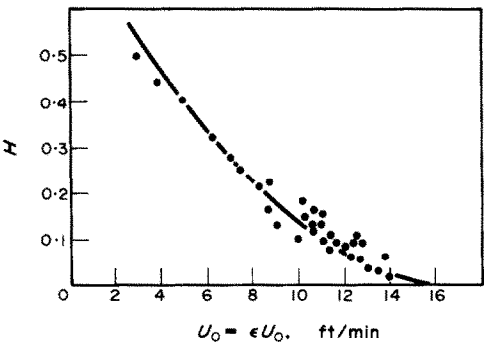

FIG. 1. Holdup vs. slip velocity.

The fluid flux, the so called superficial fluid velocity, will be

$$\tilde{u}_f = \varepsilon u_f. \tag{3}$$

Similarly, the superficial solid velocity will be

$$\tilde{u}_s = (1 - \varepsilon)u_s. \tag{4}$$

Hence we can express

$$u_0 = \frac{\tilde{u}_f}{\varepsilon} - \frac{\tilde{u}_s}{1 - \varepsilon}. \tag{5}$$

The equations (1) and (5) predict the holdup $H = 1 - \varepsilon$ if the fluid and solid fluxes are known. The equations are not restricted to the counter-current operation described above, but may be applied to any combination of $\tilde{u}_f$ and $\tilde{u}_s$ whether positive, negative or zero.

Likewise the approach explained above [3] presents another, similar approach of the fluidized bed behavior, with the main difference being that the holdup H is presented as a function of $\tilde{u}_s$.

2.2. *Particle motion*

The motion of the individual particle is random and does not lend itself easily into mathematical form. Here the research is more difficult and the publications less numerous. The information found in the literature is reviewed below.

Furukawa and Ohmae [5] compared the fluidized particles to liquid molecules and described the behavior of particles in terms of mean kinetic energy of particle. The authors measured the effective viscosity in gas fluidized beds and, basing on the molecular analogy, obtained an empirical correlation for the kinetic energy.

Ruckenstein [6] has considered the limiting case of incipient fluidization and represented the fluidized bed by a fixed lattice model where the solid particles oscillate about the fixed equilibrium position. This model is based on the analogy to the molecular behavior of solids. Ruckenstein derives a correlation for the diffusivity of fluid phase of the fluidized bed and compares it with the experimental data of others.

A more general approach was chosen by Houghton [7], whose analysis was not restricted as that of Furukawa *et al.* to gas fluidized beds, or as that of Ruckenstein to incipient fluidization. Therefore it deserves more attention. Houghton suggested a theoretical model of the particle motion which is equivalent to the Brownian motion, with the difference that the particle motion is anisotropic. He described the particle motion by means of the Langevin equation in three space directions

$$\frac{du_i}{dt} + \alpha_i u_i = S_i(t) \tag{6}$$

where α_i is a constant factor and $S_i(t)$ a stochastic term. He considered in his analysis the buoyancy forces and the mean fluid motion which exist in the vertical direction only, thus, making the particle motion anisotropic. The solution of (6) produces the particle diffusivity

$$\kappa_i = 2\frac{E_i}{m\alpha_i} \tag{7}$$

where E_i is the mean energy of particle and m the mass. Unfortunately, Houghton did not produce any valid expression of mean energy E_1 which renders his work incomplete.

2.3. *Heat transfer*

Consider the heat transfer to the single particle first. Here we have [8]

$$Nu = a + bRe^k Pr^l \tag{8}$$

where a, b, k and l are empirical constants. [8] lists the constants as determined by various investigators. For the flow conditions which apply in our case, we have

$$\left.\begin{aligned} a &\cong 2{\cdot}0 \\ b &\cong 0{\cdot}4\text{–}1{\cdot}0 \\ k &\cong 0{\cdot}5 \\ l &\cong 0{\cdot}33. \end{aligned}\right\} \tag{9}$$

Now if consider the the fluidized bed as a whole, the apparent random motion of fluidized particles introduces a considerable complexity into the heat-transfer picture. The fluid in fluidized bed has a temperature gradient as a result of the occurring heat exchange and the bulk motion of particles and fluid. The random motion of particles, being superimposed upon the fluid-temperature field, causes an irregular temperature–time pattern in the particle's ambient state; whereby the particle acts as a heat source or heat sink at random.

Amundson and Aris [9] analyzed this phenomenon on a statistical basis using a probability function for particles' distribution. Because of mathematical complexity, their solution is applicable to specific and limited cases only.

Bart in his study of gas fluidized beds described the mixing behavior of fluidized particles in terms of an effective diffusivity similar to the theory of turbulent flow (see [10]). His approach was followed by Donnadieu [11], Lewis *et al.* [12], and Borodulya and Tamarin [13], who

measured the effective thermal diffusivity caused by the particle mixing of gas fluidized beds. Thus, there exist two pertinent heat-transfer modes in a fluidized bed: first, convective heat transfer between points of the bed caused by the particle mixing and second, heat transfer between particles and fluid reviewed before. Donnadieu [14] and Littman and Barile [15] showed this by writing the energy conservation equation for the solid and fluid phases in the form

$$(1-\varepsilon)\rho_s c_s\left(\frac{\partial T_s}{\partial t}+u_s\frac{\partial T_s}{\partial x}\right)-k_s\frac{\partial^2 T_s}{\partial x^2}+h\sigma(T_s-T_f)=0 \quad (10)$$

$$\varepsilon\rho_f c_f\left(\frac{\partial T_f}{\partial t}+u_f\frac{\partial T_f}{\partial x}\right)+h\sigma(T_f-T_s)=0 \quad (11)$$

where k_s is an effective conductivity caused by particle mixing, h the particle-fluid heat transfer coefficient, ρ density, c specific heat, and σ the specific particle surface defined by

$$\sigma=6\frac{1-\varepsilon}{d}. \quad (12)$$

Now a serious question is being raised as to the validity of equation (11). It was noted [16] that the random mixing of solids in fluidized beds induces a similar mixing of fluid. Cairns and Prausnitz [17] measured this mixing in terms of diffusivity and found it to be affected by holdup. This implies that an additional conductivity term is needed in equation (11) which now becomes

$$\varepsilon\rho_f c_f\left(\frac{\partial T_f}{\partial t}+u_f\frac{\partial T_f}{\partial x}\right)-k_f\frac{\partial^2 T_f}{\partial x^2}+h\sigma(T_f-T_s)=0. \quad (13)$$

Equation (10) and (13) form a system of partial differential equations which describe the temperature field in a fluidized bed†. To solve it, one has to know the heat-transfer parameters h, k_s and k_f. Toward this end we reviewed more than twenty papers and abstracts to learn the parameters obtained by students of fluidized beds. [10, 18, 19, 40] present summarized reviews of the existing state of art.

The h values are of particular interest to us. They vary considerably from one investigator to another. This discrepancy of test results is best illustrated in a comparison study of Barker [19]. The results of his study are summarized in Fig. 2 which is taken from his paper. In the figure the heat-transfer coefficients obtained by different investigators are shown in the non-dimensional form of a Colburn factor

$$j=\frac{Nu}{Re\,Pr^{0.33}}. \quad (14)$$

The indicated Reynolds number is based upon the particle diameter d and slip velocity u_0. As seen in the figure, the test results differ by an enormous factor of 10000 (for a comparison we included a curve for a single sphere). Barker attributed the disagreement of test data to the shortcomings in technique of the individual investigators and to the differences between fluidized beds and conditions during the experiments. The majority of investigators used air as the working fluid. A few investigators used helium, argon, carbon dioxide or water. Most of them used different size particles, materials, and bed dimension. A majority considered the particle-to-fluid heat transfer to be predominant in fluidized beds, disregarding the heat exchange caused by particle mixing. Other investigators assumed the heat exchange caused by mixing to be infinite which again does not suit our purpose.

Analyzing the published heat-transfer data we found the following: In gas fluidized beds the volumetric heat capacity of the solids is of the order of about 1000 times that of the gas. Because of this, the gas rapidly attains the temperature of the solids and the heat transfer process is restricted to a narrow zone near the gas entrance to the bed. However, in liquid fluidized beds the heat capacities of the liquid and solid are of the same order of magnitude and the heat transfer occurs in the entire bed.

† Analogous equations exist for the y and z directions.

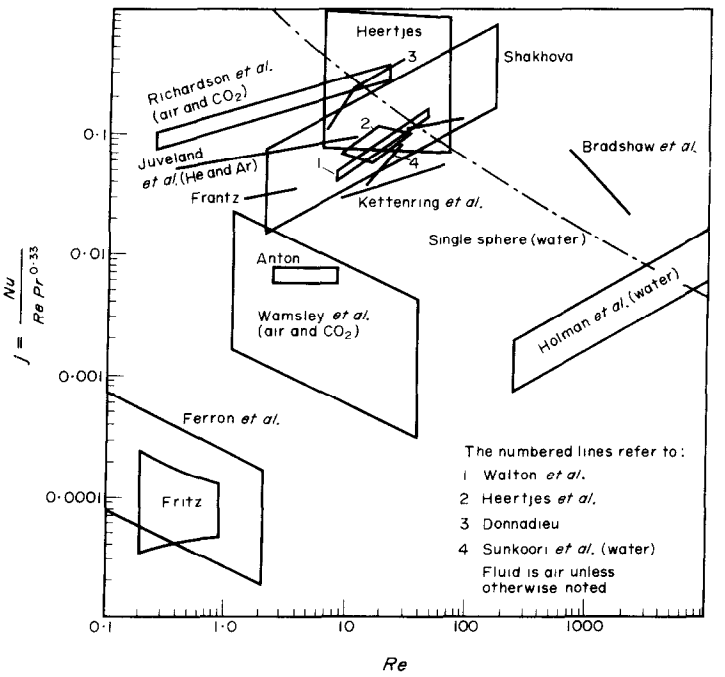

FIG. 2. Summary of heat transfer coefficients reported in the literature.

Thus there exists a specific dissimilarity between heat transfer processes in liquid and gas fluidized beds which could eventually account for some of the discrepancy of test data. To date, only two papers have been published on the subject of heat transfer in water fluidized beds [20, 21]. Because of our interest in water fluidized beds, we shall consider them separately.

Holman *et al.* [20] used a steady state method in which stainless steel and lead spheres were fluidized in water and heated by induction heating. The diameter of particles was 1·6–4·8 mm, the diameter of test column 51 mm. Thermocouples were used to measure the water temperature at the entrance and the exit to the bed and water rate was measured with a flowmeter. In their evaluation of h the authors neglected to take into consideration the heat transfer caused by mixing of solids or fluid, i.e. they assumed

$$k_s = k_f = 0. \tag{15}$$

The results were correlated by means of the equation

$$Nu = 3{\cdot}07 \,.\, 10^{-6}\, Re^2\, Pr^{1{\cdot}5} \left(\frac{D}{d}\right)^{0{\cdot}5} \left(\frac{\rho_f}{\rho_s}\right)^2 \times [1 - (1 - \varepsilon^{\frac{3}{2}} \,.\, \pi^{\frac{1}{2}} \,.\, (\tfrac{3}{4})^{\frac{3}{2}}]^{-2} \tag{16}$$

where D is the column diameter, and Re is based upon particle diameter d and slip velocity u_0.

Sunkoori and Kaparthi [21] performed transient heat transfer tests with granite and quartz particles of 0·5 and 1·1 mm dia. A batch of hot particles was dropped into an upward stream of cold water and the temperature of water leaving the bed was recorded as a function of time. The authors evaluated h assuming there were no temperature gradients in the fluidized bed, which means

$$k_s = k_f = \infty. \tag{17}$$

They correlated their results with the formula

$$Nu = 0{\cdot}00391\, Re^{2.1} \tag{18}$$

where Re has the same meaning as before. The authors predicted by means of their theory an exponential temperature distribution vs. time, a fact which contradicts the test data presented in the paper. They seem to have failed to present a valid explanation of this discrepancy.

In view of the above described contradictory information obtained on the heat-transfer data, the analysis of Mixon *et al.* [22] is of considerable interest in that it offers a valid explanation to the found discrepancies. Although intended for use in the liquid–liquid fluidized beds, it is applicable here. Mixon *et al.* start by discussing the heat-transfer coefficients h. These should be equal, within an order of magnitude, to the accepted heat transfer coefficients of single spheres, as expressed by our quation (8). Now, if one applies the accepted heat-transfer coefficients to the fluidized beds under consideration, one finds them sufficiently high to make the temperature difference $\Delta T = T_s - T_f$ in any place negligibly small when compared with the temperature drop along the column's axis. This applies, as shown by Mixon *et al.*, to fluidized beds with column length exceeding the particle sizes by two orders of magnitude or more.† Thus, in the case under consideration, there is only a single temperature

$$T_s \cong T_f = T. \tag{19}$$

Its differential equation for steady state, as derived by Mixon *et al.* equals

$$[(1-\varepsilon)\rho_s c_s u_s + \varepsilon_f c_f u_f]\frac{dT}{dx} - (k_s + k_f)\frac{d^2T}{dx^2} = 0. \tag{20}$$

It corresponds to our system of equations (10) and (13).

The expounded theory shows that it is necessary to know the effective terms $k_s + k_f$ in order to be able to determine the temperatures in fluidized bed, and the exact knowledge of the heat-transfer coefficient h is irrelevant as long as it equals or exceeds the h value for a single sphere. It also proves the h values obtained by previous investigators to be substantially inaccurate: erroneous evaluation methods were used assuming either $k_s = k_f = \infty$ or $k_s = k_f = 0$. This explains the apparent paradox of Fig. 2 that the fluidized particles seem to possess lower heat-transfer coefficients than the single spheres.

The present review will be incomplete without mentioning the work of Letan and Kehat [23]. They produced experimental heat transfer data obtained in counter-current liquid–liquid fluidized beds (spray towers). Also here was shown analytically that the heat-transfer coefficient h is irrelevant to the heat-transfer analysis of fluidized beds. The results could not be applied to the present study because of the different type of fluidized beds used.

In all, we have reviewed the heat-transfer data in three kinds of beds: solid–liquid, solid–gas and liquid–liquid. We were unable to find effective conductivity values for use in our design of a solid–water fluidized bed heat exchanger. Therefore, we started our own experimental program.

3. EXPERIMENTAL METHODS

3.1. *Test apparatus*

A counter-current fluidized bed apparatus was built on laboratory scale to obtain the needed heat-transfer data. The test apparatus was so designed as to create solid–water fluidized beds where temperatures and solid and fluid fluxes were to be identical with an industrial heat

† For benefit of the reader who is interested in quantitative data, it should be noted that for a typical solid–liquid fluidized bed the Nusselt number based upon particle diameter is of the order of 10 which makes ΔT to be about 0·5°C or less (for detailed analysis of ΔT, see [22]). This is negligibly small when compared to the temperature drop along the column which is of the order of two decades higher, see for instance Fig. 4, our typical test data.

exchanger unit. Figure 3 shows the test apparatus. The essential part is the vertical test tube 4 which contains the fluidized bed and where the heat transfer process takes place. The test tube is made of glass or Perspex which provides a visual aid in observing the fluidized bed. Its internal diameter and length can be varied.

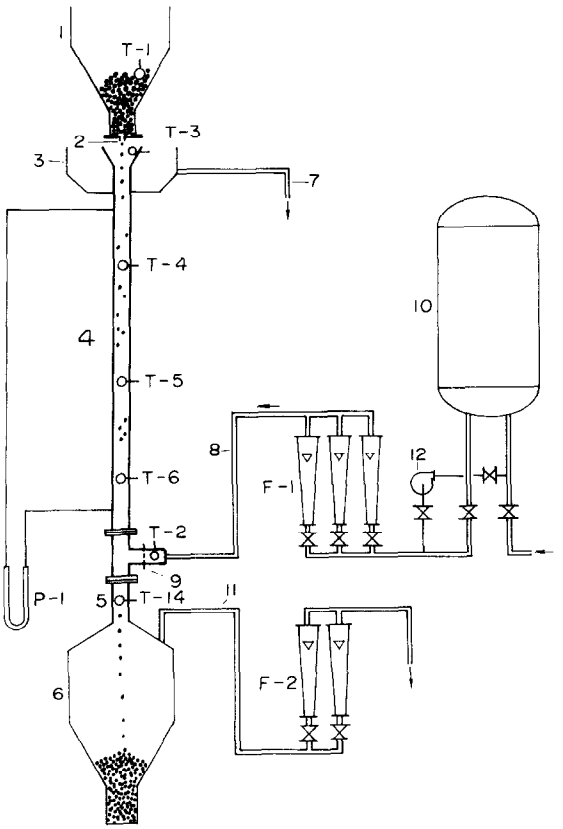

FIG. 3. Test apparatus.

Two counter-current streams pass through the test tube: an upward stream of hot water and downward stream of cold solids. The flow of solids originates in the hopper 1. From here the solids flow through the control orifice 2 into the test tube and then, through the bottom pipe 5, into the storage vessel 6. The hot water comes from the pressurized water heater 10 and is delivered through the supply line 8 into the lower part of test tube 4. Before it enters the test tube, it passes through the filter 9 whose function is to guard against penetration of fluidized solids into the supply line 8. After passing the test tube, the water gets into the overflow container 3 from where it is disposed by means of the discharge line 7. There is an additional discharge line 11, whereby water is discharged from vessel 6 while the vessel is being filled with solids. The control orifice 2 is provided with a slide valve which permits a sudden opening or closing of the orifice. 12 is a recirculation pump which is used during the preparation prior to the tests.

The following measuring devices are used in the test apparatus. The holdup is measured by means of the pressure differential gauge P-1. T-1 to T-14 are thermocouples: T-1 measures the temperature of dry solids, T-2 the temperature of entering water, T-3 to T-14 the temperature of bed. F-1 and F-2 are two sets of flowmeters. The flow rate of water is controlled by means of needle valves located next to the flowmeters. The flow of solids is controlled by the orifice 2 which is calibrated prior to the test. The flow rate of water through the discharge line 11 is set equal to the flow rate of solids through the orifice 2.

The length of the test tube was varied between 74 cm and 235 cm. The diameter was either 24 mm or 44 mm. The solids were glass spheres, 0·33, 0·71 and 3·0 mm dia. and steel spheres, 0·91 mm dia. (their properties are given in Table 1). The holdups were 4–25 per cent. Only counter-current operations were performed with the solid and fluid fluxes so adjusted that

$$\frac{G_s c_s}{G_f c_f} = 1 \tag{21}$$

where G_s and G_f are the solid and fluid rates in kg/min and c_s and c_f the specific heats. The latter condition was chosen because of its industrial application.

Table 2 shows the test readings with all the pertinent test data. The thermocouple locations x_0, x_1, x_2, etc., refer to their positions as measured from the bottom of test tube 4. The temperature

Table 1. Properties of solids

Material	Glass	Glass	Steel	Glass
Diameter, *mm*	0·25—0·40	0·59—0·84	0·84—1·0	3·0
Spec. heat, $\frac{cal}{g\tau}$	0·210	0·209	0·118	0·214
Spec. gravity, $\frac{g}{cm^2}$	2·51	2·48	7·85	2·46
Supplier	Metal Improvement Co. N.J.			E.T.E. Salvadory France

readings T_0, T_1, T_2, etc., correspond to the respective thermocouple locations. Figure 4 shows temperature readings of a typical test.

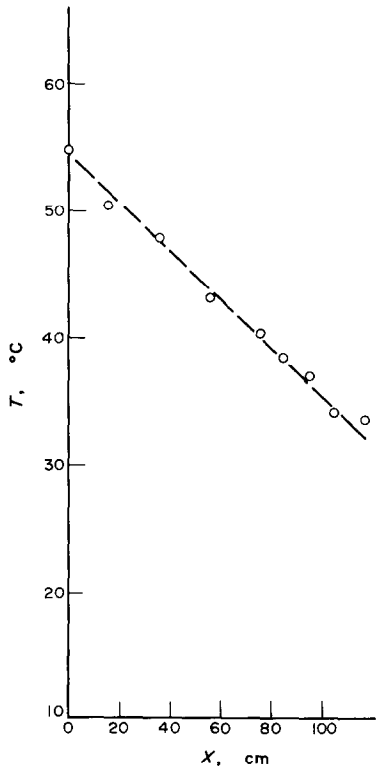

FIG. 4. Typical temperature readings.

3.2. *Data reduction*

Here we use the differential equation (20) obtained by Mixon *et al.* With some modifications it becomes

$$u_{\text{eff}} \frac{dT}{dx} - \kappa_{\text{eff}} \frac{d^2T}{dx^2} = 0 \tag{22}$$

where u_{eff} is an effective velocity term defined by the equation

$$u_{\text{eff}} = \frac{(1-\varepsilon)\rho_s c_s u_s + \varepsilon \rho_f c_f u_f}{(1-\varepsilon)\rho_s c_c + \varepsilon \rho_f c_f}$$

and κ_{eff} is the effective diffusivity defined by

$$\kappa_{\text{eff}} = \frac{k_s - k_f}{(1-\varepsilon)\rho_s c_s + \rho_f c_f}. \tag{24}$$

In the case under consideration we have $u_{\text{eff}} = 0$ as a consequence of condition (21). Because of this, equation (22) changes into

$$\frac{d^2T}{dx^2} = 0. \tag{25}$$

x is measured from the bottom of test tube 4 upward. The boundary conditions which apply here are

$$T = T_0 \quad \text{when} \quad x = 0 \tag{26}$$

$$\frac{\pi D^2}{4}(k_s + k_f)\frac{dT}{dx} = -G_s c_s (T - T_a) \quad \text{when} \quad x = L \tag{27}$$

where L is the length of the test tube and T_a the temperature of solids in hopper 1. With this the solution of the differential equation (25) will be

$$T = T_0 - (T_L - T_a) \cdot \beta \cdot \frac{x}{L} \tag{28}$$

Table 2. Test data

Test No.	19	20	21	23	24	25	26	30	31	32	33	34	51	53
Solids	glass	glass	glass	glass	glass	glass	glass	steel	steel	steel	steel	steel	glass	glass
d, mm	0·715	0·335	0·335	0·335	0·335	0·335	0·335	0·915	0·915	0·915	0·915	0·915	3·0	3·0
D, cm	4·2	4·2	4·2	4·2	4·2	4·2	4·2	2·36	2·36	2·36	2·36	2·36	2·36	2·36
L, cm	174	174	174	94	94	134	134	174	174	174	174	174	150	150
G_s/ρ_s, l/min	1·22	0·650	0·650	0·650	0·650	0·650	0·650	0·374	0·720	0·720	0·960	0·960	0·415	0·500
G_f/ρ_f, l/min	0·61	0·33	0·33	0·32	0·33	0·33	0·33	0·342	0·670	0·670	0·890	0·890	0·20	0·24
$1-\varepsilon$	0·205	0·191	0·205	0·154	0·145	0·185	0·177	0·038	0·095	0·094	0·163	0·170	0·049	0·076
x_1, cm	38	38	38	28	28	38	38	—	—	—	—	—	46	46
x_2, cm	78	78	78	38	38	78	78	—	—	—	—	—	86	86
x_3, cm	118	118	118	48	48	—	—	—	—	—	—	—	—	—
T_0, °C	49·5	48·0	46·0	46·3	51·0	44·0	47·3	46·0	61·4	60·5	63·9	63·9	42·8	42·1
T_1, °C	44·0	42·1	40·7	41·6	45·8	39·0	40·9	—	—	—	—	—	39·7	39·3
T_2, °C	41·1	37·5	36·9	40·5	44·5	34·2	35·5	—	—	—	—	—	36·9	35·8
T_3, °C	32·6	34·5	33·0	39·3	42·6	—	—	—	—	—	—	—	—	—
T_L, °C	27·7	28·7	27·7	31·8	33·2	27·2	28·5	25·2	20·3	23·5	19·6	18·5	32·5	30·5
T_a, °C	24·3	25·7	25·3	28·3	27·3	24·3	24·8	19·6	18·0	21·0	17·4	15·8	27·7	28·5
β	6·44	5·77	6·92	3·86	3·02	5·79	5·08	4·00	17·9	14·8	20·1	16·7	2·15	5·30
κ_{eff}, cm^2/s	21·0	12·5	10·4	9·6	12·5	9·5	10·8	57·5	24·9	30·1	29·6	29·6	59·1	29·7
Re^*	141	44·7	42·6	48·1	53·6	42·7	46·0	405	331	332	281	272	1050	1608

Test No.	54	55	56	57	58	59	60	61	62	63	64	66	67	68
Solids	glass	glass	glass	glass	glass	glass	glass	glass	glass	glass	glass	glass	glass	glass
d, mm	0·715	0·715	0·715	0·715	0·335	0·335	0·335	0·335	0·335	0·335	0·335	0·335	0·335	0·335
D, cm	2·36	2·36	2·36	2·36	2·36	2·36	2·36	2·36	2·36	2·36	2·36	2·36	2·36	2·36
L, cm	150	150	150	150	150	150	150	150	150	150	150	150	150	150
G_s/ρ_s, l/min	0·234	0·288	0·335	0·145	0·214	0·162	0·162	0·169	0·188	0·191	0·104	0·209	0·104	0·104
G_f/ρ_f, l/min	0·13	0·136	0·158	0·080	0·100	0·080	0·08	0·085	0·089	0·090	0·060	0·100	0·060	0·060
$1-\varepsilon$	0·098	0·140	0·174	0·042	0·249	0·151	0·140	0·151	0·204	0·219	0·083	0·242	0·087	0·079
x_1, cm	46	46	46	46	46	46	46	46	46	46	46	26	26	26
x_2, cm	86	86	86	86	86	86	86	86	86	86	86	46	46	46
x_3, cm	—	—	—	—	—	—	—	—	—	—	—	66	66	6
x_4, cm	—	—	—	—	—	—	—	—	—	—	—	86	86	86
T_0, °C	42·3	—	—	431	410	—	—	44·0	43·9	35·4	—	34·5	30·5	—
T_1, °C	39·8	41·0	416	40·0	48·0	43·8	41·7	40·9	39·6	33·8	38·6	32·8	30·1	38·6
T_2, °C	36·7	37·8	37·4	373	35·0	31·6	36·6	37·0	35·0	32·0	35·5	32·3	30·1	37·6
T_3, °C	—	—	—	—	—	—	—	—	—	—	—	31·6	29·7	35·7
T_4, °C	—	—	—	—	—	—	—	—	—	—	—	31·1	29·5	34·7
T_L, °C	32·7	31·3	30·9	33·2	30·2	29·7	31·5	32·0	29·0	30·0	31·3	27·7	39·0	31·8
T_a, °C	29·2	28·7	26·5	29·2	28·5	28·4	28·7	29·0	25·5	28·2	26·5	26·1	27·4	29·0
β	2·86	5·58	3·50	2·45	6·53	3.46	4·82	4·45	4·26	3·00	2·31	4·00	0·875	2·79
κ_{eff}, cm^2/s	25·7	16·6	31·2	18·1	11·1	15·1	10·8	12·2	14·6	21·3	14·8	17·7	37·1	11.6
Re^*	174	159	146	230	39·2	42·8	49·6	42·8	41·4	38·4	55·8	35·7	49·0	58·2

Test No.	69	70	71	72	73	74	75	77	78	79	80	81	82	83
Solids	glass	glass	glass	glass	glass	glass	glass	glass	glass	glass	glass	glass	glass	glass
d, mm	0·715	0·715	0·715	3·0	3·0	0·335	0·335	0·335	0·335	0·335	0·335	0·335	3·0	0·715
D, cm	2·36	2·36	2·36	2·36	2·36	2·36	2·36	2·60	2·60	2·60	2·60	2·60	2·50	2·60
L, cm	150	150	150	150	150	150	150	115	115	115	115	115	115	115
G_s/ρ_s, l/min	0·290	0·208	0·146	0·507	0·402	0·192	0·165	0·159	0·167	0·192	0·212	0·103	0·504	0·205
G_f/ρ_f, l/min	0·140	0·100	0·070	0·240	0·190	0·091	0·078	0·075	0·079	0·091	0·100	0·060	0·240	0·097
$1-\varepsilon$	0·158	0·087	0·053	0·083	0·057	0·242	0·189	0·135	0·135	0·188	0·240	0·073	0·063	0·073
x_1, cm	26	26	26	26	26	26	26	14·5	14·5	14·5	14·5	14·5	14·5	14·5
x_2, cm	46	46	46	46	46	46	46	29·0	29·0	29·0	29·0	29·0	29·0	29·0
x_3, cm	66	66	66	66	66	66	66	43·5	43·5	43·5	43·5	43·5	43·5	43·5
x_4, cm	86	86	86	86	86	86	86	58·0	58·0	58·0	58·0	58·0	58·0	58·0
T_0, °C	—	36·2	33·5	—	—	—	—	—	—	—	—	—	—	—
T_1, °C	35·5	35·7	32·7	37·1	39·0	32·9	30·7	30·3	31·1	32·5	31·8	35·9	35·7	30·5
T_2, °C	35·2	34·7	32·0	36·1	37·5	32·1	30·4	30·3	30·5	31·8	31·5	34·4	34·2	29·9
T_3, °C	33·7	33·7	31·6	34·8	35·9	31·4	29·7	29·4	29·6	30·9	30·6	33·3	32·5	28·6
T_4, °C	32·8	32·8	30·7	33·5	34·1	30·7	29·1	29·1	28·7	30·2	30·4	32·3	31·4	28·0
T_L, °C	29·0	30·5	29·0	30·6	28·5	28·7	27·0	28·0	27·0	28·0	28·4	29·9	28·2	26·2
T_a, °C	26·0	27·6	25·4	26·8	24·8	26·5	25·1	27·0	24·3	25·5	26·6	25·3	25·5	24·0
β	2·83	2·68	1·25	3·65	3·51	3·69	2·25	2.60	2·00	1·96	2·22	1·71	3·77	2·24
κ_{eff}, cm^2/s	33·2	24·2	35·8	43·2	35·2	17·6	24·1	12·2	16·6	20·1	20·1	11·7	25·6	17·7
Re^*	133	165	239	1455	1700	40·2	36·9	41·3	41·3	38·5	35·5	55·2	1569	156

Test No.	84	85	86	87	88	89	90	91	92	93	94	95	96
Solids	glass	glass	glass	glass	glass	glass	glass	glass	glass	glass	glass	glass	glass
d, mm	0·335	0·335	0·335	0·335	3·0	3·0	0·335	0·335	3·0	3·0	0·715	0·715	0·335
D, cm	2·36	2·36	3·85	3·85	3·85	3·85	2·60	2·60	2·60	2·60	2·6	2·60	2·60
L, cm	115	115	117	117	117	117	235	235	235	235	235	235	235
G_s/ρ_s, l/min	0·159	0·159	0·291	0·530	0·905	2·00	0·093	0·189	0·487	0·878	0·151	0·298	0·216
G_f/ρ_f, l/min	0·077	0·077	0·153	0·285	0·477	1·05	0·049	0·099	0·256	0·462	0·078	0·155	0·114
$1-\varepsilon$	0·115	0·115	0·079	0·211	0·050	0·150	0·051	0·147	0·058	0·158	0·048	0·093	0·161
x_1, cm	14·5	14·5	16·0	16·0	16·0	16·0	46·0	46·0	46·0	46·0	46·0	46·0	46·0
x_2, cm	29·0	29·0	35·0	36·0	36·0	36·0	75·0	75·0	75·0	75·0	75·0	75·0	75·0
x_3, cm	43·5	43·5	56·0	56·0	56·0	56·0	104·0	104·0	104·0	104·0	104·0	104·0	104·0
x_4, cm	58·0	58·0	76·0	76·0	76·0	76·0	133·0	133·0	133·0	133·0	133·0	133·0	133·0
x_5, cm	77·0	77·0	95·0	95·0	95·0	95·0	162·0	162·0	162·0	162·0	162·0	162·0	162·0
x_6, cm	102·0	102·0	105·0	105·0	10·50	105·0	212·0	212·0	212·0	212·0	212·0	212·0	212·0
T_0, °C	48·4	32·3	52·3	50·8	54·6	69·0	42·4	45·0	51·4	50·4	40·6	47·0	52·0
T_1, °C	46·0	31·5	49·2	47·9	50·4	61·0	35·4	39·8	43·6	46·0	36·8	43·0	46·4
T_2, °C	43·9	31·0	46·6	45·2	47·8	56·0	33·0	36·8	41·4	42·5	34·4	41·2	43·0
T_3, °C	41·4	30·4	41·6	40·5	43·1	46·6	29·6	33·0	38·0	40·0	32·0	38·4	39·6
T_4, °C	39·1	29·9	32·2	36·7	40·2	39·4	28·2	31·0	35·7	36·8	30·2	36·4	37·2
T_5, °C	35·5	29·3	32·5	29·6	36·9	28·6	25·6	28·0	32·0	33·2	28·4	34·4	34·0
T_6, °C	33·0	28·5	31·4	27·6	34·0	25·8	22·2	22·8	25·6	23·6	26·0	29·8	282
T_L, °C	32·3	28·0	28·6	26·5	33·5	25·6	20·0	20·6	21·6	20·6	24·0	27·2	25·2
T_a, °C	26·0	25·4	15·7	14·8	14·3	14·8	14·2	16·0	16·4	16·0	18·3	22·0	20·5
β	3·00	1·54	2·06	2·31	1·28	5·40	2·91	4.91	4·29	6·53	2.52	3.11	4.42
κ_{eff}, cm^2/s	10·5	20·4	12·9	22·2	63·7	35·0	12·4	15·8	44·4	554	23·3	38·2	20·1
Re^*	54·5	44·7	64·8	44·5	2050	1516	60·0	43·2	1560	1260	196	177	48·7

where T_L is the bed temperature at $x = L$ and β is defined by the equation

$$\beta = \frac{G_s c_s L}{k_s + k_f} \cdot \frac{4}{\pi D^2}. \tag{29}$$

From the test we get temperature readings T_0, T_L and T_v ($v = 1, 2, \ldots$) where T_v values correspond to thermocouples' locations x_v. Upon insertion into equation (28), they should produce β which then can be used to evaluate $k_s + k_f$. But the actual value T_0, T_L and T_v deviate from equation (28), because of instrumentation errors and discrepancy between the idealized theory and experiments. Because of this, the last squares method is used to evaluate β.

$$S = \sum_1^m (\Delta T_v)^2 = \sum_1^m \left\{T_v - \left[T_0 - (T_L - T_a)\beta \frac{x_v}{L}\right]\right\}^2 \tag{31}$$

where m is the number of temperature readings. One finds the values of β, T_0, T_L by solving the system of equations

$$\frac{\partial S}{\partial \beta} = 0 \tag{32}$$

$$\frac{\partial S}{\partial T_0} = 0 \tag{33}$$

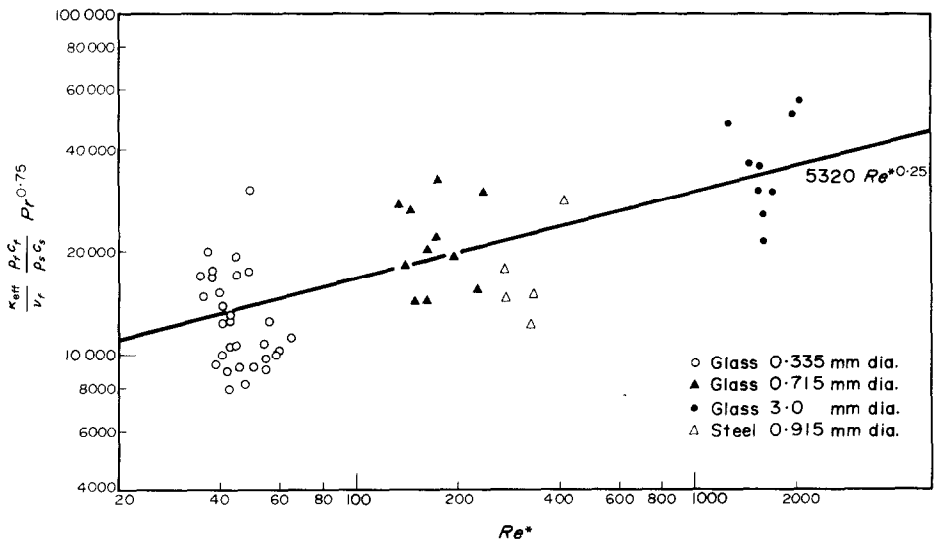

FIG. 5. Test results.

The deviation of T_v from its theoretical value is

$$\Delta T_v = T_v - \left[T_0 - (T_L - T_a) . \beta . \frac{x_v}{L}\right]. \tag{30}$$

The sum of squares of ΔT_v equals

and

$$\frac{\partial S}{\partial T_L} = 0. \tag{34}$$

This we did by method of function minimization of Regev [24].

3.3. *Test results*

We plotted our test results to indicate the trend. Once the results fell into an accepted range, we proceeded to develop a theoretical model to explain this trend. The theoretical model is described in Sections 4 and 5. The final formula is

$$\frac{\kappa_{\text{eff}}}{v_f} = C \cdot \frac{\rho_s c_s}{\rho_f c_f} \frac{Re^{*0.25}}{Pr^{0.75}} \tag{35}$$

where the Reynolds number Re^* is defined by equation (89). C is a proportionality constant, the value of which was the missing link in our model. By fitting the test data and using the least squares method it was found that

$$C = 5320. \tag{36}$$

Figure 5 shows graphically the relation between the test data and the above formula. The standard deviation of the scatter was calculated and found to be ± 34 per cent.

4. DIFFUSION OF HEAT IN A FLUIDIZED BED

Our theoretical model aims to explain the nature of effective conduction in fluidized beds. Mixon *et al.* [22] showed successfully this phenomenon to be predominant in heat transfer in fluidized beds, but did not give sufficient theory. Our theoretical explanation follows.

The conduction is a result of the solid mixing which resembles the eddy motion of turbulent fluid flow. This resemblance is especially evident visually to an observer of fluidized bed in motion. We follow the methods of the theory of turbulent flow to determine this conduction. For simplification's sake, we accept the "perfectly mixed drop" model of fluidized particles, i.e. we assume the conductivity of particle material to be infinite and the particles do not possess internal temperature gradients. As for the fluid, we ignore its molecular diffusion: the latter is negligible when compared to the turbulent diffusion.

We express the velocities and temperatures in fluidized bed by means of the sums of the mean values and the fluctuation terms, i.e.

$$u_{s,i} = \overline{u}_{s,i} + u'_{s,i} \tag{37}$$

$$u_{f,i} = \overline{u}_{f,i} + u'_{f,i} \tag{38}$$

$$T_s = \overline{T}_s + T'_s \tag{39}$$

$$T_f = \overline{T}_f + T'_f \tag{40}$$

where index i denotes the space directions, and s and f designate the solid and fluid respectively. $u_{s,i}$ and $u_{f,i}$ are vectors. Any part of the fluidized bed is subject to the energy conservation law. In the form known to the reader from the turbulent theory, it becomes

$$(1-\varepsilon)\rho_s c_s \left[\frac{\partial \overline{T}_s}{\partial t} + \overline{u}_{s,i}\frac{\partial \overline{T}_s}{\partial x_i} + \frac{\partial}{\partial x_i}(\overline{T'_s u'_{s,i}})\right] + \varepsilon\rho_f c_f \left[\frac{\partial \overline{T}_f}{\partial t} + \overline{u}_{f,i}\frac{\partial \overline{T}_f}{\partial x_i} + \frac{\partial}{\partial x_i}(\overline{T'_f u'_f})\right] = 0 \tag{41}$$

where the respective values ρ, c and $\bar{u}$ are assumed to be constant. In writing equation (41) we use the summation convention whereby repeated subscripts mean summation. Equation (41) expresses our view that the heat exchange takes place by means of convection only and the molecular diffusion of fluid is ignored.

Several simplifications are in order before we proceed with the analysis of (41). First, we assume the difference $\Delta\overline{T} = \overline{T}_s - \overline{T}_f$ to be very small when compared to the measurable temperature differences between various points of fluidized bed. This subject was discussed at length by Mixon *et al.* [22] who showed this to be so in industrial fluidized bed, i.e. if $\overline{T}_s$ and $\overline{T}_f$ and their first space- and time-derivatives are continuous and monotonous functions of x_i and t which we expect them to be, the derivatives of $\Delta\overline{T}$ will be negligibly small and one can write

$$\frac{\partial \overline{T}_s}{\partial t} \cong \frac{\partial \overline{T}_f}{\partial t} = \frac{\partial \overline{T}}{\partial t} \tag{42}$$

and

$$\frac{\partial \bar{T}_s}{\partial x_i} \cong \frac{\partial \bar{T}_f}{\partial x_i} = \frac{\partial \bar{T}}{\partial x_i} \tag{43}$$

skipping the index s and f for brevity. Consider now the vectors $\overline{T'_s u'_{s,i}}$ and $\overline{T'_f u'_{f,i}}$. Both have the character of a heat flux. Consider $\overline{T'_s u'_{s,i}}$ first. It represents a heat flux caused by particle mixing. Following the methods of Boussinesq [25] and Schmidt [26]. we make the assumption that it is proportional to the mean temperature gradient, i.e.

$$\overline{T'_s u'_{s,i}} = -\kappa_s \frac{\partial \bar{T}}{\partial x_i} \tag{44}$$

where κ_s is a proportionality constant. The constant, of course, may differ in each direction x_i, thus the general form will be

$$\overline{T'_s u'_{s,i}} = -\kappa_{s,ij} \frac{\partial \bar{T}}{\partial x_j} \tag{45}$$

where $\kappa_{s,ij}$ is a tensor. As for $T'_f u'_{f,i}$, it represents the heat flux caused by fluid mixing. Here

$$\overline{T'_f u'_{f,i}} = -\kappa_{f,ij} \frac{\partial \bar{T}}{\partial x_j} \tag{46}$$

where $\kappa_{f,ij}$ is another constant tensor. Combining equations (41) and (46) we obtain

$$[(1-\varepsilon)\rho_s c_s + \varepsilon\rho_f c_f]\frac{\partial \bar{T}}{\partial t} + [(1-\varepsilon)\rho_s c_s \bar{u}_{s,i} + \varepsilon\rho_f c_f \bar{u}_{f,i}]\frac{\partial \bar{T}}{\partial x_i} - [(1-\varepsilon)\rho_s c_s \kappa_{s,ij} + \varepsilon\rho_f c_f \kappa_{f,ij}]\frac{\partial^2 \bar{T}}{\partial x_i \partial x_j} = 0. \tag{47}$$

It is equivalent to equation (20) which was derived formerly by Mixon *et al.* Upon putting

$$\bar{u}_{\text{eff},i} = \frac{(1-\varepsilon)\rho_s c_s \bar{u}_{s,i} + \varepsilon\rho_f c_f \bar{u}_{f,i}}{(1-\varepsilon)\rho_s c_s + \varepsilon\rho_f c_f} \tag{48}$$

and

$$\kappa_{\text{eff},ij} = \frac{(1-\varepsilon)\rho_s c_s \kappa_{s,ij} + \varepsilon\rho_f c_f \kappa_{f,ij}}{(1-\varepsilon)\rho_s c_s + \varepsilon\rho_f c_f} \tag{49}$$

we finally obtain

$$\frac{\partial \bar{T}}{\partial t} + \bar{u}_{\text{eff},i}\frac{\partial \bar{T}}{\partial x_i} - \kappa_{\text{eff},ij}\frac{\partial^2 \bar{T}}{\partial x_i \partial x_j} = 0. \tag{50}$$

The latter is the thermal diffusion equation of fluidized bed.

Because of its importance to heat-transfer analysis, equation (50) deserved more attention. The mean temperature $\bar{T}$ can be expressed by means of the probability function $p(x, t)$. It can be shown (see the next chapter) that equation (50) is equivalent to

$$\frac{\partial p(x,t)}{\partial t} + \bar{u}_{\text{eff},i}\frac{\partial p(x,t)}{\partial x_i} - \kappa_{\text{eff},ij}\frac{\partial^2 p(x,t)}{\partial x_i \partial x_j} = 0. \tag{51}$$

Now the latter is a particular form of the Kolmogorov's forward equation of stochastic processes. Consequently we can consider the heat-transfer process in fluidized bed as a Weiner process.

Here we refer to the Houghton paper [7]. Houghton was the first to suggest a Wiener process model for fluidized beds. Although he considered the particles' motion and not the heat transfer, some of his results also apply here. In the next chapter we shall derive the effective diffusivity from the existing solution of Wiener processes.

5. EFFECTIVE DIFFUSIVITY

We consider the heat-transfer process of a single particle. With certain simplifying assumptions it becomes a Wiener process. From the theory of Wiener processes we will find the effective diffusivity to be a function of the mean kinetic energy of particle and the heat-transfer coefficient. In what follows, we shall develop the expressions for the kinetic energy and the heat transfer coefficient, and apply it to obtain the correlation of the effective diffusivity.

5.1. *The Wiener process*

We observe the random behavior of fluidized particles using the Lagrangian system, i.e. we mark each particle by means of parameter $\boldsymbol{x} = (x_1, x_2, x_3)$ and follow the particle along the coordinates $\boldsymbol{X} = (X_1, X_2, X_3)$ and t. Parameter $\boldsymbol{x}$ is the position of particle at time $t = t_0$. The particle's velocity in Lagrangian term is

$$\boldsymbol{U}(\boldsymbol{x}, t) = \frac{\partial}{\partial t}\boldsymbol{X}(\boldsymbol{x}, t). \tag{52}$$

As shown by Houghton [7], the behavior of an individual particle can be described approximately by the Langevin equation

$$m\frac{\mathrm{d}^2 X_i}{\mathrm{d}t^2} + f\frac{\mathrm{d}X_i}{\mathrm{d}t} = F_i'(t) \tag{53}$$

where m is the particle's mass, f a friction factor and $F_i'(t)$ a stochastic term. To circumvent the difficulties impending the solution of equation (53) and described at length by Houghton, we make several simplifying assumptions at the expense of accuracy. The assumptions are: first, say that the fluidized bed is isotropic, and neglect the influence of walls and buoyancy; second, we assume equipartition of energy; third, we say that the collision process is purely random. The third assumption means that

$$\overline{F_i(t)\,F_i(s)} = 0 \quad \text{when} \quad t \neq s \tag{54}$$

and

$$\overline{F_i(t\,F_i(s)} = \text{const.} = 2m\bar{E} \quad \text{when} \quad t = s \tag{55}$$

where $\bar{E}$ is the mean energy of particle (see [27]–[29]). In conjunction with the above assumptions, the behavior of fluidized particles can be explained by means of the theory of Brownian motion.

Consider the heat transfer in the light of the explained particle behavior. The heat balance can be described by the differential equation

$$V\rho_s c_s\frac{\mathrm{d}T_s}{\mathrm{d}t} + Ah(T_s - T_f) = 0 \tag{56}$$

where V is the volume of the particle and A its surface. As will be explained later in subsection 5.3, the heat transfer takes place by means of heat dissipation eddies. The thickness of the thermal boundary layer surrounding the particle corresponds to the size of the eddies. Outside the boundary layer the heat is already dissipated and the temperature is substantially uniform, i.e. equal $\overline{T}_f$. In view of this, the above equation has to be corrected to read

$$V\rho_s c_s\frac{\mathrm{d}T_s}{\mathrm{d}t} + Ah(T_s - \overline{T}_f) = 0. \tag{56'}$$

By differentiating the latter in respect to time and expressing T_s in terms of its mean and fluctuation components, one obtains

$$V\rho_s c_s\frac{\mathrm{d}^2 T_s'}{\mathrm{d}t^2} + Ah\frac{\mathrm{d}T_s'}{\mathrm{d}t} = -V\rho_s c_s\frac{\mathrm{d}^2\overline{T}_s}{\mathrm{d}t^2} - Ah\frac{\mathrm{d}}{\mathrm{d}t}(\overline{T}_s - \overline{T}_f). \tag{57}$$

Here, the last right term equals zero by virtue of (42) and (43). The remaining term equals

$$-V\rho_s c_s\frac{\mathrm{d}^2\overline{T}_s}{\mathrm{d}t^2} = \frac{\mathrm{d}}{\mathrm{d}t}\left(-V\rho_s c_s\frac{\mathrm{d}\overline{T}_s}{\mathrm{d}t}\right) = K'(t) \tag{58}$$

where $K'(t)$ denotes the time derivative

$$\frac{\mathrm{d}}{\mathrm{d}t}[K(t)]$$

From here we obtain the Langevin equation

$$-V\rho_s c_s\frac{\mathrm{d}^2 T_s'}{\mathrm{d}t^2} + Ah\frac{\mathrm{d}T_s'}{\mathrm{d}t} = K'(t). \tag{59}$$

Function $K(t)$ is stochastic because it depends upon the random particle motion. In the fluidized bed under consideration, during the steady state, the mean temperature gradient is constant because of the precondition (21). During the transient condition, even that the error is about ± 1 per cent, we still take it as a constant. This makes $K(t)$ equal

$$K(t) = -V\rho_s c_s\frac{\mathrm{d}\overline{T}_s}{\mathrm{d}t} = -V\rho_s c_s\frac{\mathrm{d}\overline{T}_s}{\mathrm{d}X_i}\cdot\frac{\mathrm{d}X_i}{\mathrm{d}t} = -V\rho_s c_s\frac{\mathrm{d}\overline{T}_s}{\mathrm{d}X_i}U_i \tag{60}$$

and its correlation function equal

$$\overline{K(t)K(s)} = 0 \quad \text{when} \quad t \neq s \tag{61}$$

and

$$\overline{K(t)K(s)} = \left(V\rho_s c_s \frac{\mathrm{d}\bar{T}_s}{\mathrm{d}X_i}\right)^2 . \overline{U_i^2} = \text{const.} \quad \text{when} \quad t = s. \tag{62}$$

Equations (59), (61) and (62) make the heat transfer a Wiener process.

As a result of all that has been considered up to now, we see that the particle motion and particle heat transfer both are expressed by the same Langevin equations (53) and (59), and both can be classified as Wiener processes. Therefore we propose by means of the existing Wiener process solutions to solve the heat-transfer problem.

Equation (59) can be brought into the more convenient form

$$\frac{\mathrm{d}^2 T_s'}{\mathrm{d}t^2} + \gamma \frac{\mathrm{d}T_s'}{\mathrm{d}t} = \phi'(t) \tag{63}$$

where

$$\gamma = \frac{Ah}{V\rho_s c_s} \tag{64}$$

and

$$\phi'(t) = \frac{K'(t)}{V\rho_s c_s}. \tag{65}$$

Its approximate solution, as shown in [30], is the Gaussian probability function

$$p(T_s', t) = \frac{1}{(4\pi\chi t)^{\frac{1}{2}}} \exp\left(-\frac{T_s'^2}{4\pi t}\right). \tag{66}$$

where χ is the diffusivity factor defined by

$$\chi = \frac{\overline{\left(\frac{\mathrm{d}T_s'}{\mathrm{d}t}\right)^2}}{\gamma} = \frac{\overline{U_i^2}}{\gamma}\overline{\left(\frac{\mathrm{d}T_s'}{\mathrm{d}X_i}\right)^2}. \tag{67}$$

Now the object of the present analysis is the probability function $p(x, t)$ which we get from (66) by means of the transformation

$$p(\boldsymbol{X}, t) = p(T_s', t) . \left|\frac{\mathrm{d}T_s'}{\mathrm{d}\boldsymbol{X}}\right| . \tag{68}$$

see [31].

Now consider T_s' and X_i as defined by the equations (53) and (59) respectively. Between collisions, the stochastic terms $F'(t)$ and $K'(t)$ equal zero and both equations are similar e.g. T_s' and X_i are both exponental functions of t with their respective exponents proportional to the heat transfer factor Ah and the friction factor f. Following the Reynolds analogy, we assume the friction mechanism and the heat transfer of the particle to be equivalent. The assumption implies that Ah is proportional to f and

$$\frac{\mathrm{d}T_s'}{\mathrm{d}X_i} = \text{const.} \tag{69}$$

Consequently, if $\boldsymbol{x}$ is the particle location at the initial time $t = t_0$, the probability function $p(\boldsymbol{X}|\boldsymbol{x}, t)$ will have the Gaussian distribution†

$$p(\boldsymbol{X}, t) = p(\boldsymbol{X}|\boldsymbol{x}, t) = \frac{1}{(4\pi\kappa t)^{\frac{3}{2}}} . \exp\left[-\frac{(X_i - x_i)^2}{4\kappa t}\right] \tag{70}$$

where κ is the diffusivity factor

$$\kappa = \frac{\overline{U_i^2}}{\gamma} = \frac{V\rho_s c_s}{Ah} . \frac{2\bar{E}}{m}. \tag{71}$$

$p(\boldsymbol{X}|\boldsymbol{x}, t)$ satisfies the Kolmogorov's forward equation

$$\frac{\partial}{\partial t} p(\boldsymbol{X}|\boldsymbol{x}, t) - \kappa \frac{\partial^2}{\partial X_i^2} p(\boldsymbol{X}|\boldsymbol{x}, t) = 0. \tag{72}$$

If we express the mean temperature $\bar{T}(\boldsymbol{X}, t)$ by means of $p(\boldsymbol{X}|\boldsymbol{x}, t)$ so that

$$\bar{T}(\boldsymbol{X}, t) = \int_{-\infty}^{+\infty} T_s(\boldsymbol{x}, t) . p(\boldsymbol{X}|\boldsymbol{x}, t) . \mathrm{d}\boldsymbol{x} \tag{73}$$

we find that equation (72) is equivalent to

$$\frac{\partial \bar{T}}{\partial t} - \kappa \frac{\partial^2 \bar{T}}{\partial X_i^2} = 0. \tag{74}$$

† As follows from equations (66), (68) and (69).

The details of this are given in Appendix.

Returning to equation (71), the diffusivity factor κ is a function of mean energy $\bar{E}$ and heat-transfer coefficient h. In the following subsections we shall derive the expressions for $\bar{E}$ and h.

5.2. *Mean energy of particle*

We assume the fluidized bed to be isotropic, the energy of the particles to be subject to equipartition law and the particles to be spherical.

Each particle is subject to fluctuating forces which comprise weight, drag, and collision forces. The first is constant, the other two are random. The mean resultant of all forces equals

$$\bar{P} = W + D = \frac{\pi d^3}{6}(\rho_s - \rho_f) - c_D \frac{\pi d^2}{4} \rho_f \frac{u_0^2}{2g} \tag{75}$$

where W is the particle's weight in fluid, D the drag, c_D the drag coefficient and u_0 the slip velocity (the mean collision force equals zero, hence, it is dropped from the equation).

The mean energy of particle equals

$$\bar{E} = \frac{\overline{pV_B}}{N} \tag{76}$$

where p is the pressure, V_B the volume of fluidized bed, N the number of particles in volume V_B. Since the pressure is statistically independent of V_B/N, equation (76) becomes

$$\bar{E} = \bar{p}\left(\overline{\frac{V_B}{N}}\right) = \bar{p} \cdot \frac{\pi d^3}{6} \cdot \frac{1}{1-\varepsilon}. \tag{77}$$

The mean pressure is

$$\bar{p} = \frac{P}{\frac{\pi d^2}{4}} = \frac{\frac{\pi d^3}{6}\rho_s - \rho_f) - c_D \frac{\pi d^2}{4} \rho_f \frac{u_0^2}{2g}}{\frac{\pi d^2}{4}}. \tag{78}$$

From here the mean kinetic energy equals

$$\bar{E} = -\left[\frac{\pi d^3}{6}(\rho_s - \rho_i) - c_D \frac{\pi d^2}{4} \rho_f \frac{u_0^2}{2g}\right] \cdot \frac{2}{3} \cdot \frac{d}{1-\varepsilon}. \tag{79}$$

The latter equation is considerably simplified if we use the empirical correlation which we derived from the tests of Wilhelm and Kwauk [32]. Wilhelm and Kwauk made a thorough investigation of fluidized beds in 7·5 and 15 cm dia. columns. The solids were spherical particles of sand, glass, silicate catalyst and lead, ranging from 0·3 to 5 mm dia. Fluids were air and water. To suit our purpose, we confined the evaluation of their tests to water fluidized beds only. Upon plotting the test data as shown in Fig. 6, we obtained the empirical correlation

$$\frac{\pi d^3}{6}(\rho_s - \rho_f) - c_D \frac{\pi d}{4} \rho_f \frac{u_0^2}{2g} = 1{\cdot}1 \frac{\pi d^3}{6}(\rho_s - \rho_f) \cdot (1-\varepsilon)^{0.33} \tag{80}$$

where the c_D values correspond to single spheres. Equation (80) simplifies our expression of $\bar{E}$. Combined with (79), it produces

$$\bar{E} = 0{\cdot}734 \frac{\pi d^3}{6}(\rho_s - \rho_f) \cdot \frac{d}{(1-\varepsilon)^{0.67}}. \tag{81}$$

From equation (81) one can obtain the root mean square of the fluctuation velocity of the particle. It equals

$$(\sqrt{\overline{U_i^2}}) = \sqrt{\left(\frac{2\bar{E}}{m}\right)} = 1{\cdot}21 \frac{(gd)^{0.5}}{(1-\varepsilon)^{0.33}} \left(1 - \frac{\rho_f}{\rho_s}\right)^{0.5} = (\sqrt{\overline{u_i^2}}). \tag{82}$$

5.3. *The heat-transfer coefficient*

In analyzing the heat transfer to fluidized particles, most authors assume the interestitial flow to be laminar in character and independent of time. The analysis is based upon an assumed steady state velocity profile in the fluid. Contrary to these assumptions, experience has

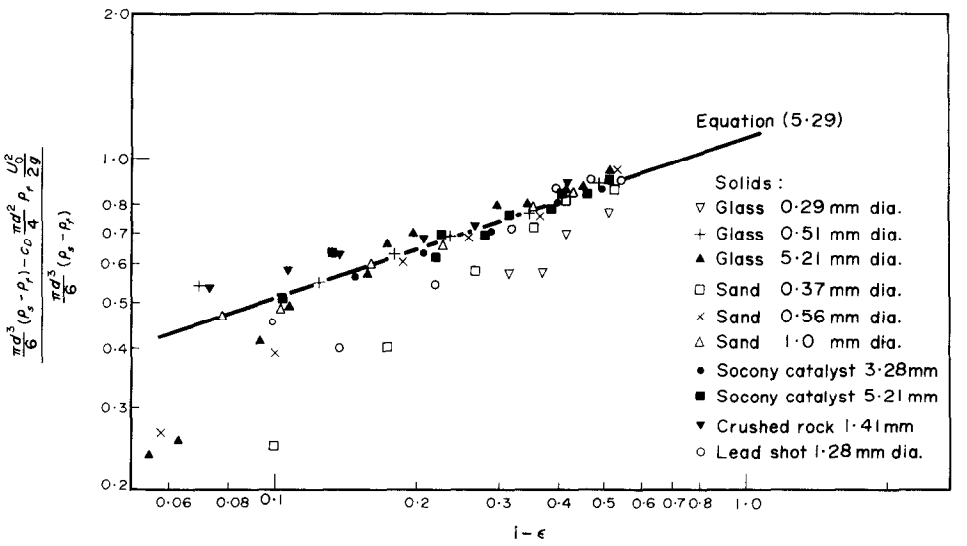

FIG. 6. Mean particle force vs. holdup.

shown the flow to be of fluctuating character and filled with turbulent eddies. Hence the old theories prove to be inadequate and one must turn to new phenomenological theories when calculating the heat transfer to the fluctuating particles.

[33] lists several phenomenological theories that are applicable to the turbulent flow under consideration. The most suitable is the penetration theory which was first introduced in [34] and [35]. The theory assumes the turbulent eddies to penetrate the liquid film surrounding the solid body.

From the above, a physical model is derived that is based on the following assumptions. First, the flow ambient to the particle is turbulent and the turbulent motion reaches the particle's surface. Second, the turbulence is isotropic. The latter assumption, i.e. isotropic turbulence near the wall, is made to utilize the existing correlations deduced for the isotropic turbulent flow from the statistical theory. It is done in similar analyses, as for example in [36]. (The validity of correlations in the vicinity of wall that were derived for isotropic turbulence—e.g. the Kolmogorov's 2/3 law—was confirmed experimentally by others. Such validity is, of course, of empirical nature only, since the correlations were derived assuming complete isotropy.)

We use Kolmogorov's 2/3 law of isotropic turbulence as applied to the heat dissipation. The latter application was demonstrated by Yaglom [37] who applied it to the temperature field of isotropic turbulence and obtained the 2/3 temperature law

$$\overline{[T(x+l)-T(x)]^2} \sim l^{\frac{2}{3}} \tag{83}$$

where the left hand term represents the second order temperature moment and l is the distance between observed temperature fluctuations. Obukhov [38] obtained the same result by non-dimensional reasoning. A direct consequence of this law is the determination of the heat dissipation length

$$\delta \sim \left(\frac{\kappa_m^3}{l}\right)^{0.25} = \frac{l}{(Re\,.\,Pr)^{0.75}} \tag{84}$$

derived by Obukhov [38], and corresponding directly to Kolmogorov's microscale

$$\delta_1 \sim \left(\frac{\nu_m^3}{l}\right)^{0.25} = \frac{l}{Re^{0.75}} \tag{85}$$

(the index m above means molecular and the Reynolds number is based on the length l).

The heat-transfer coefficient around the fluidized particle equals

$$h = \frac{k_{\text{eff}}}{\Delta x} \tag{86}$$

where k_{eff} is the effective conductivity caused by heat-transfer eddies (not to be confused with the effective conductivity of fluidized bed discussed before) and Δx is the heat absorbing layer thickness surrounding the particle. Now $\Delta x \sim \delta$. We also assume the heat transfer eddies to equal the viscous dissipation eddies, i.e.

$$\kappa_{\text{eff}} = \frac{k_{\text{eff}}}{\rho_f c_f} \cong \nu_{\text{eff}} = u' \,.\, l. \tag{87}$$

This produces the Nusselt number

$$Nu = \frac{hl}{k_m} = \text{const.} \;\; (Re \,.\, Pr)^{1\cdot 75} \tag{88}$$

where both Nu and Re are based upon the eddy size l. Since the latter varies in a direct proportion to particle size d, the same equation (88) applies if we replace l by d. The velocity used in equation (88) is the root mean square of the particle's fluctuation velocity ($\sqrt{u_i'^2}$), so that

$$Re = Re^* = \frac{(\sqrt{u_i'^2}) \,.\, d}{\nu_f}. \tag{89}$$

Combining the equations (71), (81), (88) and (89), we obtain the final correlation for the effective thermal diffusivity of fluidized bed

$$\frac{\kappa_{\text{eff}}}{\nu_f} = C \,.\, \frac{\rho_s c_s}{\rho_f c_f} \frac{Re^{*0\cdot 25}}{Pr^{0\cdot 75}} \tag{90}$$

where C is a proportionality constant to be determined experimentally. As shown in Section 3, it equals 5320. The correlation fits well into our test data, as was shown in Section 3. In Section 6 we make a comparison with the experimental data of others.

6. COMPARISON OF OUR RESULTS WITH OTHERS' TESTS

From the numerous literature reviewed we chose to check against equation (90) those tests that were conducted with water–solid fluidized beds. The results of the following investigators were used: Cairns and Prausnitz [17], Holman *et al.* [20]†, Letan [39]‡ and Sunkoori and Kaparthi [21]. The results of the comparison are shown in Fig. 7.

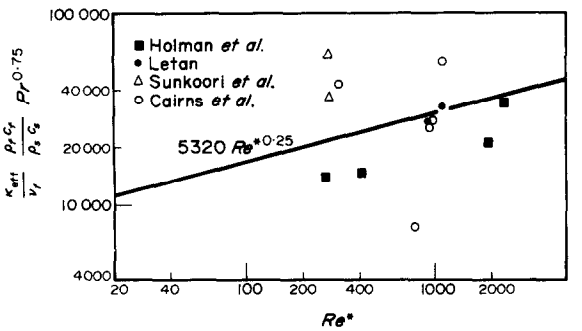

FIG. 7. Correlation of results of present work with test data of other investigators.

In the figure notice the data of Cairns *et al.* The tests are of particular interest because the subject of research was the mass transfer and the effective mass conduction, and not the heat transfer as in the others. As seen in the figure, the data of Cairns *et al.* follow the same pattern which shows that the particle's heat transfer and mass transfer are equivalent.

7. CONCLUSIONS

An experimental investigation of heat transfer in solid–water fluidized beds by means of steady state tests was conducted. The solids were 0·3–3·0 mm dia., glass and steel; the holdups were 4–25 per cent. It was found that the experimental data could be correlated by means of the semi-

† Our evaluation was based on transient data shown in the reference.

‡ By kind permission of Dr. R. Letan.

empirical equation, developed later in our theoretical analysis

$$\frac{\kappa_{\text{eff}}}{\nu_f} = C \cdot \frac{\rho_s c_s}{\rho_f c_f} \cdot \frac{Re^{*0.25}}{Pr^{0.75}} \tag{90}$$

where κ_{eff} is the effective thermal conductivity of fluidized bed, C an empirical constant, and Re^* Reynolds number, based on the particle's diameter and the root mean square fluctuation velocity defined by equation

$$(\sqrt{u_i'^2}) = 1{\cdot}21 \frac{(gd)^{0.5}}{(1-\varepsilon)^{0.33}} \cdot \left(1 - \frac{\rho_f}{\rho_s}\right)^{0.5}. \tag{82}$$

After plotting the test data, the value $C = 5320$ was obtained. The experimental data fitted equation (90) with a standard deviation ± 34 per cent.

An analysis of the heat transfer caused by particle mixing was performed by means of the theory of stochastic processes. Taking the heat transfer process as a Wiener process and using the existing solution of the Wiener processes it was shown that the effective thermal diffusivity of solid–liquid fluidized bed can be expressed by equation (90). The derivation of (90) was facilitated by assuming the fluidized bed to be isotropic and the kinetic energy of particles to be subject to equipartition law. Also it was assumed the fluidized bed to be counter-current with $G_s c_s \cong G_f c_f$.

REFERENCES

1. A. KOGAN, Process and apparatus for effecting heat transfer, U.S. Patent No. 3,242,975 (March 29, 1966).
2. L. LAPIDUS and J. C. ELGIN, Mechanics of vertical-moving fluidized systems, *A.I.Ch.E.Jl* **3** (1), 63 (1957).
3. T. S. MERTES and H. B. RHODES, Liquid–particle behavior, *Chem. Engng. Prof.* **51**, 429 (1955).
4. B. G. PRICE, L. LAPIDUS, and J. C. ELGIN, Mechanics of vertical-moving fluidized systems, *A.I.Ch.E. Jl* **5**, 93 (1959).
5. J. FURUKAWA, and T. OHMAE, Liquid-like properties of fluidized systems, *Ind. Engng Chem.* **50**, 821 (1958).
6. E. RUCKENSTEIN, Homogeneous fluidization, *I/EC Fundamentals* **3**, 260 (1964).
7. G. HOUGHTON, Particle and Fluid diffusion in homogeneous fluidization, *I/EC Fundamentals* **5**, 153 (1966).
8. S. SIDEMAN, Direct contact heat transfer between immiscible liquids, *Advances in Chemical Engineering*, Vol. 6. Academic Press, New York (1966).
9. N. R. AMUNDSON and R. ARIS, Heat transfer in fluidized and moving beds, *Proc. Third Congress of European Federation of Chem. Engng.* Instn. Chem. Engrs, London (1962).
10. M. LEVA, *Fluidization*. McGraw-Hill, New York (1959).
11. G. A. DONNADIEU, Study of particle circulation in a fluid, *J. Rech. Centre Natl Rech. Sci.*, No. 53. 295 (1960).
12. W. K. LEWIS, E. R. GILLILLAND and H. GIROUARD, Heat transfer and solids mixing in beds of fluidized solids, *Chem. Engng Prog. Symp. Ser.* **58**(38), 87 (1962).
13. V. A. BORODULYA and A. I. TAMARIN, Study of the effective thermal diffusivity of a fluidized bed, *Int. Chem. Engng* **5** (3), 432 (1965).
14. G. A. DONNADIEU, Study of heat exchange between fluid and solid particles in a fluidized bed. *J. Rech. Centre Natl Rech. Sci.* No. 51, 161 (1960).
15. H. LITTMAN and R. G. BARILE, The effects of solids mixing in fluidized bed, *Chem. Engng Prog. Symp. Ser.* **62**(67), 10 (1966).
16. P. N. ROWE, Discussion, *Proc. Third Congress of European Federation of Chem. Engng.* Instn. Chem. Engrs, London (1962)
17. E. J. CAIRNS and J. M. PRAUSNITZ, Longitudinal mixing in fluidization, *A.I.Ch.E. Jl* **6**, 400 (1960).
18. J. F. FRANTZ, Fluid to particle heat transfer in fluidized beds, *Chem. Engng. Prog.* **57** (7), 35 (1961).
19. J. J. BARKER, Heat transfer in fluidized beds, *Ind. Engng Chem.* **57** (5), 33 (1965).
20. J. P. HOLMAN, T. W. MOORE and V. M. WONG, Experimental study of particle-fluid heat transfer in a water fluidized system, Rep. NYO-10702, O.T.S., U.S. Dept. of Commerce (1963); see also *I/CE Fundamentals* **4**, 21 (1966).
21. N. R. SUNKOORI and R. KAPARTHI, Heat transfer studies between particles and liquid medium in a fluidized bed, *Chem. Engng Sci.* **12**, 166 (1960).
22. F. O. MIXON, D. R. WHITAKER and J. C. ORCUTT, Axial dispersion and heat transfer in liquid–liquid spray towers, *A.I.Ch.E. Jl* **13**, 21 (1967).
23. R. LETAN and E. KEHAT, Mechanism of heat transfer in a spray column heat exchanger, *A.I.Ch.E. Jl* **14**, 398 (1968).
24. J. REGEV, Modified gradient minimization method, *Proc. National Conference on Data Processing*. Inform. Processing Assoc. of Israel, Jerusalem (1968).
25. J. BOUSSINESQ, *Theorie de l'Ecoulement Tourbillonnant*, I-II. Gauthier-Villars, Paris (1897).
26. W. SCHMIDT, Massenaustausch bei der ungeordneten Strömung, *Sitzungber. Akad. Wiss. Wien, Math-nat.* Kl (2a) **126**, 757 (1917).
27. G. E. UHLENBECK and L. S. ORNSTEIN, On the theory of Brownian motion, *Phys. Rev.* **36**, 823 (1930). Reprinted in collection cited [30].
28. M. C. WANG and G. E. UHLENBECK, On the theory of Brownian motion, *Rev. Mod. Phys.* **17**, 323 (1945). Reprinted in collection cited in [30].
29. A. M. YAGLOM, *Introduction to the Theory of Stationary Random Functions*. Prentice Hall, Englewood Cliffs, N.J. (1965).

30. S. CHANDRASEKHAR, Stochastic problems in physics and astronomy, *Rev. Mod. Phys.* **15**, 1 (1943). Reprinted in *Selected Papers on Noise and Stochastic Processes*, edited by N. WAX. Dover, New York (1954).
31. E. PARZEN, *Modern Probability Theory and its Applications*, p. 323. John Wiley, New York (1960).
32. R. H. WILHELM and M. KWAUK, Fluidization of solid particles, *Chem. Engng Prod.* **44**, 209 (1948).
33. R. S. BRODKEY, *The Phenomena of Fluid Motions*, pp. 602–603. Addison-Wesley, Reading, Mass. (1967).
34. P. V. DANCKWERTS, Significance of liquid-film coefficients in gas absorption, *Int. Engng Chem.* **43**, 1460 (1951).
35. T. J. HANRATTY, Turbulent exchange of mass and momentum with a boundary, *A.I.Ch.E. Jl* **2**, 359 (1956).
36. V. G. LEVICH, *Physicochemical Hydrodynamics*. Prentice Hall, Englewood Cliffs, N.J. (1962).
37. A. M. YAGLOM, On local structure of temperature field in turbulent flow, *Dokl. Akad. Nauk S.S.S.R.* **69**, 743 (1949) Reprinted in Translation cited in [38].
38. A. M. OBUKHOV, Structure of temperature field in a turbulent flow, *Izv. Akad. Nauk. S.S.S.R. Sr. Geograf i Geofiz.* **13**, 58 (1949). German Translation in *Sammelband zur Statistischen Theorie der Turbulenz*, edited by H. Goering. Akademie Verlag, Berlin (1958).
39. R. LETAN, Personal Communication.
40. S. S. ZADBRODSKY, *Hydrodynamics and Heat Transfer in Fluidized Beds*. MIT Press, Cambridge, Mass. (1966).

APPENDIX

Derivation of Thermal Diffusion Equation

The mean temperature is defined by

$$\overline{T}(X,t) = \int_{-\infty}^{+\infty} T_s(x,t)\,.\,p(X|x,t)\,.\,\mathrm{d}x. \tag{A.1}$$

Its partial time derivative is

$$\frac{\partial \overline{T}}{\partial t} = \int_{-\infty}^{+\infty} \frac{\partial T_s}{\partial t}\,.\,p(X|x,t)\,.\,\mathrm{d}x + \int_{-\infty}^{+\infty} T_s\,.\,\frac{\partial}{\partial t}p(X|x,t)\,.\,\mathrm{d}x. \tag{A.2}$$

Now

$$\int_{+\infty}^{+\infty} \frac{\mathrm{D}T_s}{\mathrm{D}t}\,.\,p(X|x,t)\,.\,\mathrm{d}x,$$

the mean value of the derivative following the motion of the particle temperature, is given by

$$\int_{-\infty}^{+\infty} \frac{\mathrm{D}T_s}{\mathrm{D}t}\,.\,p(X|x,t)\,.\,\mathrm{d}x = \int_{-\infty}^{+\infty} \left\{\frac{\partial T_s}{\partial t} + U_i\frac{\partial T_s}{\partial X_i}\right\}.\,p(X|x,t)\,.\,\mathrm{d}x$$

$$= \int_{-\infty}^{+\infty} \frac{\partial T_s}{\partial t}\,.\,p(X|x,t)\,.\,\mathrm{d}x + \int_{-\infty}^{+\infty} U_i\frac{\partial T_s}{\partial X_i}\,.\,p(X|x,t)\,.\,\mathrm{d}x. \tag{A.3}$$

Considering

$$\int_{-\infty}^{+\infty} U_i\frac{\partial T_s}{\partial \overline{X}_i}\,.\,p(X|x,t)\,\mathrm{d}x,$$

we see that using the transformation

$$\int_{-\infty}^{+\infty} p(U|x,t) = \left|\frac{\mathrm{d}X_i}{\mathrm{d}U_i}\right|\,.\,p(X|x,t),$$

it becomes

$$\int \frac{\partial T_s}{\partial X_i}\,.\left|\frac{\mathrm{d}X_i}{\mathrm{d}U_i}\right|^{-1}\,.\,U_i(x,t)\,.\,p(U|x,t)\,.\,\mathrm{d}x$$

which is zero, since

$$\frac{\partial T_s}{\partial X_i} = \frac{\partial \overline{T}}{\partial X_i} + \frac{\partial T_s'}{\partial X_i} = \text{const.} \tag{A.4}$$

$$\left|\frac{\mathrm{d}X_i}{\mathrm{d}U_i}\right| = \text{const.} \tag{A.5}$$

and the mean value of the particle velocity following the motion

$$\overline{U}_i = \int_{-\infty}^{+\infty} U_i(x,t)\,.\,p(U|x,t)\,.\,\mathrm{d}x = 0. \tag{A.6}$$

(Note: equation (A.4) follows from the experimental work described; equation (A.5) follows from the fact that both distribution functions, $p(\overline{X}|x,t)$ and $p(U|x,t)$ are expressed by equivalent Gaussians, see [30].) Then

$$\int_{-\infty}^{+\infty} \frac{\partial T_s}{\partial t}\,.\,p(X|x,t)\,.\,\mathrm{d}x = \int_{-\infty}^{+\infty} \frac{\mathrm{D}T_s}{\mathrm{D}t}\,.\,p(X|x,t)\,.\,\mathrm{d}x. \tag{A.7}$$

The heat transfer equation for the particle may be written as

$$\int_{-\infty}^{+\infty} \frac{\mathrm{D}T_s}{\mathrm{D}t}\,.\,p(X|x,t)\,.\,\mathrm{d}x = -\gamma\int_{-\infty}^{+\infty} (T_s - \overline{T}_f)\,.\,p(X|x,t)\,.\,\mathrm{d}x$$

$$= -\gamma\int_{-\infty}^{+\infty} T_s'\,.\,p(T_s'|x,t)\,.\left|\frac{\mathrm{d}T_s'}{\mathrm{d}X}\right|\,.\,\mathrm{d}x \tag{A.8}$$

so

$$\int_{-\infty}^{+\infty} \frac{\partial T_s}{\partial t}\,.\,p(X|x,t)\,.\,\mathrm{d}x = -\gamma\int_{-\infty}^{+\infty} T_s'\,.\,p(T_s'|x,t)\,.\left|\frac{\partial T_s'}{\mathrm{d}X}\right|\,.\,\mathrm{d}x = 0 \tag{A.9}$$

since T_s' is a completely random function. Hence

$$\frac{\partial \overline{T}}{\partial t} = \int_{-\infty}^{+\infty} T_s\,.\,\frac{\partial}{\partial t}p(X|x,t)\,.\,\mathrm{d}x. \tag{A.10}$$

The second space derivative of $\overline{T}$ equals

$$\frac{\partial^2 \bar{T}}{\partial X_i^2} = \frac{\partial}{\partial X_i} \int_{-\infty}^{+\infty} \frac{\partial T_s}{\partial X_i} \cdot p(\boldsymbol{X}|\boldsymbol{x}, t) \cdot \mathrm{d}\boldsymbol{x} + \frac{\partial}{\partial X_i} \int_{-\infty}^{-\infty} T_s \cdot \frac{\partial}{\partial X_i} p(\boldsymbol{X}|\boldsymbol{x}, t) \cdot \mathrm{d}\boldsymbol{x}. \quad \text{(A.11)}$$

The first right term of this equation is a derivative of a constant, hence equals zero. The second right term becomes

$$\frac{\partial}{\partial X_i} \int_{-\infty}^{+\infty} T_s \cdot \frac{\partial}{\partial X_i} p(\boldsymbol{X}|\boldsymbol{x}, t) \cdot \mathrm{d}\boldsymbol{x} = \int_{-\infty}^{+\infty} \frac{\partial T_s}{\partial X_i} \cdot \frac{\partial}{\partial X_i} p(\boldsymbol{X}|\boldsymbol{x}, t) \cdot \mathrm{d}\boldsymbol{x} + \int_{-\infty}^{+\infty} T_s \cdot \frac{\partial^2}{\partial X_i^2} p(\boldsymbol{X}|\boldsymbol{x}, t) \cdot \mathrm{d}\boldsymbol{x} \quad \text{(A.12)}$$

where

$$\int_{-\infty}^{+\infty} \frac{\partial T_s}{\partial X_i} \cdot \frac{\partial}{\partial X_i} p(\boldsymbol{X}|\boldsymbol{x}, t) \cdot \mathrm{d}\boldsymbol{x} = \frac{\partial T_s}{\partial X_i} \cdot \frac{\partial}{\partial X_i} \int_{-\infty}^{+\infty} p(\boldsymbol{X}|\boldsymbol{x}, t) \cdot \mathrm{d}\boldsymbol{x} = 0. \quad \text{(A.13)}$$

This makes

$$\frac{\partial^2 \bar{T}}{\partial X_i^2} = \int_{-\infty}^{+\infty} T_s \cdot \frac{\partial^2}{\partial X_i^2} p(\boldsymbol{X}|\boldsymbol{x}, t) \cdot \mathrm{d}\boldsymbol{x}. \quad \text{(A.14)}$$

The probability function $p(\boldsymbol{X}|\boldsymbol{x}, t)$ satisfies the equation

$$\frac{\partial}{\partial t} p(\boldsymbol{X}|\boldsymbol{x}, t) - \kappa \frac{\partial^2}{\partial X_i^2} p(\boldsymbol{X}|\boldsymbol{x}, t) = 0. \quad \text{(A.15)}$$

In conjunction with equation (A.10) and (A.14) the latter becomes

$$\frac{\partial \bar{T}}{\partial t} - \kappa \frac{\partial^2 \bar{T}}{\partial X_i^2} = 0. \quad \text{(A.16)}$$

TRANSFERT THERMIQUE DANS DES LITS FLUIDISÉS LIQUIDES

Résumé—Il existe deux modes de transfert thermique dans un lit fluidisé: l'un est le transfert thermique convectif entre des points du lit, causé par le mélange des particules, et l'autre est le transfert thermique superficiel entre les particules et le fluide. Les deux modes produisent une convection ou une diffusion thermique effective dans le lit fluidisé. Afin de prédire les températures dans le lit fluidisé, il est nécessaire de connaître la diffusivité thermique effective. Les objectifs atteints de la présente recherche sont (a) l'explication théorique du transfert thermique et (b) la détermination expérimentale de la diffusivité mentionnée.

Le travail est divisé en deux parties principales, l'une expérimentale et l'autre théorique. Dans la partie expérimentale les valeurs de la diffusivité thermique effective sont obtenues au moyen d'un montage à lit fluidisé. Les valeurs obtenues répondent à la corrélation semi-empirique développée dans notre analyse théorique:

$$\frac{\kappa_{\text{eff}}}{\nu_f} = C \cdot \frac{\rho_s c_s}{\rho_f c_f} \cdot \frac{Re^{*0{\cdot}25}}{Pr^{0{\cdot}75}}$$

où Re^* est un nombre de Reynolds basé sur le diamètre de particule et la racine carrée de la moyenne quadratique de la fluctuation de vitesse définie par l'équation:

$$(\sqrt{u'^2}) = 1{\cdot}21 \frac{(gd)^{0{\cdot}5}}{(1-\varepsilon)^{0{\cdot}33}} \cdot \left(1 - \frac{\rho_f}{\rho_s}\right)^{0{\cdot}5}.$$

C est un facteur de proportionnalité. En reportant sur un graphique les résultats des essais on trouve $C = 5320$. Les résultats répondent à l'équation ci-dessus avec une déviation standard de ± 34 pour cent.

Dans la partie théorique du travail, une analyse du transfert thermique causé par le mélange des particules est conduite au moyen de la théorie des processus stochastiques. On montre qu'avec certaines hypothèses simplificatrices le processus du transfert thermique devient un processus de Wiener. A partir de la théorie des processus de Wiener on trouve que la diffusivité thermique effective du lit fluidisé est une fonction de l'énergie cinétique moyenne de la particule, et du coefficient de transfert thermique. On développe, pour compléter l'analyse, les expressions de l'énergie cinétique moyenne de la particule et le coefficient de transfert thermique. Ces deux expressions en accord avec la théorie des processus de Wiener conduisent à la corrélation semi-empirique citée auparavant.

WÄRMEÜBERTRAGUNG IN FLÜSSIGEN FLIESSBETTEN

Zusammenfassung—Es gibt zweierlei Arten der Wärmeübertragung in Fliessbetten: Einmal die konvektive Wärmeübertragung zwischen verschiedenen Stellen des Bettes, verursacht durch die Mischbewegungen; zum anderen die Wärmeübertragung von der Oberfläche der Partikel an das Fluid. Diese zweierlei Arten ergeben zusammen eine effektive Wärmeleitung oder Diffusion im Fliessbett. Um die Temperaturverteiling

im Fliessbett vorauszuberechnen, benötigt man die Kenntnis der effektiven Warmeleitfähigkeit. Die Ergebnisse der vorliegenden Untersuchung sind:
(a) theoretische Erklärung des Wärmeübergangs; (b) experimentelle Bestimmung des effektiven Wärmetransports.
Die Arbeit gliedert sich in zwei Hauptteile, einen experimentellen und einen theoretischen. Im experimentellen Teil sind Werte des effektiven Wärmetransports mit Hilfe einer Fliessbett-Versuchsapparatur ermittelt. Diese Werte bestätigen die halbempirische Beziehung, die im theoretischen Teil abgeleitet wird,

$$\frac{k_{\text{eff}}}{\nu_f} = C\frac{\rho_s c_s}{\rho_f c_f}\cdot\frac{Re^{*0,25}}{Pr^{0,75}}$$

wobei Re^* eine Reynoldszahl ist, die mit dem Partikeldurchmesser und der Wurzel aus dem mittleren Geschwindigkeitsquadrat gebildet wird mit

$$\sqrt{(\overline{u'^2})} = 1{,}21\frac{(gd)^{0,5}}{(1-\varepsilon)^{0,33}}\cdot\left(1-\frac{\rho_f}{\rho_s}\right)^{0,5};$$

C ist ein Proportionalitätsfaktor. Durch Auftragung der Versuchsergebnisse wurde $C = 5320$ ermittelt. Die Versuchsergebnisse stimmen mit der obigen Gleichung mit einer Abweichung von $\pm$ 34 Prozent überein.
Im theoretischen Teil der Arbeit wurde eine Analyse des Wärmetransports, der durch die Partikelbewegung verursacht wird, mit Hilfe der Theorie der stochastischen Prozesse durchgeführt. Es wird gezeigt, dass mit einigen vereinfachenden Annahmen der Vorgang des Wärmetransports zu einem Wiener-Prozess wird. Ausgehend von der Theorie für den Wiener-Prozess ergibt sich, dass der effektive Wärmetransport des Fliessbettes eine Funktion der mittleren kinetischen Energie der Partikel und der Wärmeleitfähigkeit ist. Um die Analyse zu ergänzen, wurden Ausdrücke für die mittlere kinetische Energie der Partikel und für die Wärmeleitfähigkeit abgeleitet. Beide Ausdrücke in Verbindung mit der Theorie für Wiener-Prozesse ergeben die oben angegebene halbempirische Beziehung.

ТЕПЛООБМЕН В СЛОЯХ, ПСЕВДООЖИЖЕННЫХ КАПЕЛЬНОЙ ЖИДКОСТЬЮ

Аннотация—В псевдоожиженном слое существует два рода переноса тепла: конвективный теплообмен между точками слоя, вызванный перемешиванием частиц и поверхностный теплообиен между частицами и средой. Оба вызывают эффективную теплопроводность или диффузию тепла в псевдоожиженном слое. Для того, чтобы рассчитать температуру в псевдоожиженном слое, необходимо знать эффективную температуропроводность. Данное исследование имело две цели: теоретическое объяснение теплообмена и экспериментальное определение эффективной температуропроводности.

Работа делится на две основные части: экспериментальную и теоретическую. В экспериментальной части значения эффективной температуропроводности получены на экспериментальных установках с псевдоожиженным слоем. Полученные значения обобщаются полуэмпирическим соотношением, выведенным в теоретической части

$$\frac{\kappa_{\text{eff}}}{\nu_f} = C\frac{\rho_s c_s}{\rho_f c_f}\cdot\frac{Re^{*0,25}}{Pr^{0,75}}$$

где Re^*—число Рейнольдса, отнесенное к диаметру частицы и среднеквадратичной скорости пульсации, определяемой уравнением

$$(\sqrt{u'^2}) = 1{,}21\frac{(gd)^{0,5}}{(1-\epsilon)^{0,33}}\cdot\left(1-\frac{\rho_f}{\rho_s}\right)^{0,5}$$

где C—коэффициент пропорциональности. При графическом представлении экспериментальных данных найдено, что $C = 5320$. Экспериментальные данные обобщаются с помощью этого уравнения со стандартным отклонением $\pm 34\%$.

В теоретической части с помощью теории стохастических процессов проводится анализ теплообмена, вызванного перемешиванием частиц. Показано, что при определенных упрощениях процесс теплообмена сводится к винеровскому процессу. Из теории винеровских процессов найдено, что эффективная температуропроводность псевдоожиженного слоя есть функция средней кинетической энергии частицы и коэффициента теплообмена. Анализ завершен выводом выражений средней кинетической энергии частицы и коэффициента теплообмена. Оба выражения совместно с теорией винеровских процессов дают полуэмпирическую корреляцию, приведенную выше.